HHS Public Access

Author manuscript

Acta Biomater. Author manuscript; available in PMC 2018 April 17.

Published in final edited form as:

Acta Biomater. 2018 January ; 65: 53–65. doi:10.1016/j.actbio.2017.10.046.

Synthesis and evaluation of dual crosslinked alginate microbeads

Sami I. Somo[a,c], **Kelly Langert**[a,c], **Chin-Yu Yang**[b], **Marcella K. Vaicik**[a,c], **Veronica Ibarra**[a], **Alyssa A. Appel**[a], **Banu Akar**[a,c], **Ming-Huei Cheng**[b,*], and **Eric M. Brey**[a,e,d]

[a]Department of Biomedical Engineering, Illinois Institute of Technology, Chicago, IL, USA

[b]Center for Tissue Engineering, Chang Gung Memorial Hospital, Taoyuan, Taiwan

[c]Research Service, Edward Hines, Jr. VA. Hospital, Hines, IL, USA

[d]Department of Biomedical Engineering, University of Texas at San Antonio, San Antonio, TX, USA

[e]Research Service, Audie L. Murphy Memorial VA Hospital, San Antonio, TX, USA

Abstract

Alginate hydrogels have been investigated for a broad variety of medical applications. The ability to assemble hydrogels at neutral pH and mild temperatures makes alginate a popular choice for the encapsulation and delivery of cells and proteins. Alginate has been studied extensively for the delivery of islets as a treatment for type 1 diabetes. However, poor stability of the encapsulation systems after implantation remains a challenge. In this paper, alginate was modified with 2-aminoethyl methacrylate hydrochloride (AEMA) to introduce groups that can be photoactivated to generate covalent bonds. This enabled formation of dual crosslinked structure upon exposure to ultraviolet light following initial ionic crosslinking into bead structures. The degree of methacrylation was varied and *in vitro* stability, long term swelling, and cell viability examined. At low levels of the methacrylation, the beads could be formed by first ionic crosslinks followed by exposure to ultraviolet light to generate covalent bonds. The methacrylated alginate resulted in more stable beads and cells were viable following encapsulation. Alginate microbeads, ionic (unmodified) and dual crosslinked, were implanted into a rat omentum pouch model. Implantation was performed with a local injection of 100 μl of 50 μg/ml of Lipopolysaccharide (LPS) to stimulate a robust inflammatory challenge *in vivo*. Implants were retrieved at 1 and 3 weeks for analysis. The unmodified alginate microbeads had all failed by week 1, whereas the dual-crosslinked alginate microbeads remained stable up through 3 weeks. The modified alginate microbeads may provide a more stable alternative to current alginate-based systems for cell encapsulation.

*Corresponding author at: Division of Microsurgery Reconstructive Micro-surgery, Department of Plastic and Reconstructive Surgery, Chang Gung Memorial Hospital, 5, Fu-Hsing Street Kueishan, Taoyuan 33305, Taiwan. minghuei@cgmh.org.tw (M.-H. Cheng).

Disclosure statement

No competing financial interests exist.

Keywords

Alginate; Microbeads; Methacrylated alginate; Inflammation; Omentum

1. Introduction

Alginate hydrogels have received considerable attention for use in medical applications, including drug delivery, stem cell culture, tissue engineering, and cell encapsulation [1–3]. The success of alginate-based hydrogels in biomedical applications results, in part, from the expected stability of the material. In drug delivery and cell encapsulation systems, the stability of the hydrogel contributes to the success of sustained delivery of functional cells or solutes. Therefore, the ability to design a successful alginate system is dependent on the stability of the hydrogel to resist degradation following implantation.

Alginate is a naturally occurring polysaccharide that is capable of undergoing ionic crosslinking in the presence of divalent cations [4]. Cells can be immobilized within the alginate when ionic bridges are formed between neighboring mannuronic and guluronic groups, trapping the cells within the crosslinked polymer mesh. Prior to gelation, the cells are suspended within the dissolved alginate, and upon exposure to the cation, a hydrogel network forms around the cells. Unlike many other gelation procedures, this crosslinking can occur at pH, temperature and salt conditions that maintain cell viability and/or protein activity. When combined with this straightforward technique for crosslinking, alginate has become a popular material for cell-based therapies [5].

Cell encapsulation within alginate microbeads is utilized to prevent graft rejection of non-autologous cell transplants. Alginate has been studied extensively for the delivery of islets as a treatment for type 1 diabetes [2,6,7]. Microencapsulation has been shown to result in prolonged survival and function of islet grafts in chemically induced and autoimmune diabetic animal models [8–11]. In addition, clinical trials have shown some success with regards to decreased exogenous insulin requirements [12]. However, results with regard to the length of graft survival and overall metabolic benefits have varied. Differences in study outcomes are difficult to interpret as they might arise from the use of different capsule material/condition, islet source, implantation sites, and recipients [12].

A primary reason for graft failure is the breakdown of the microbead material rather than poor cell function. The material can fail in response to an inflammatory challenge or mechanical stress. Implantation of a foreign material induces an inflammatory response [13–15]. This inflammatory response results in the growth and differentiation of immune cells and fibroblasts around the capsule which may disrupt the transport of nutrients, leading to death of the encapsulated cells. In addition, inflammatory cells may also contribute to breakdown down of the alginate due to increased cytokine production [16]. In addition to the implant-associated inflammatory response, depending on the location of implantation the stability of the alginate can be disrupted by local mechanical stresses [17]. For example, beads implanted within the peritoneal cavity experience different mechanical stresses compared to those implanted within the omentum. Increasing stability of alginate

microbeads upon exposure to an inflammatory challenge and mechanical stress could improve clinical outcomes.

Covalent crosslinks can be introduced to improve the stability of alginate. Carboxylate groups present on the monomer chains provide a region for relatively straight forward modification and has been used to attach fluorescence markers [18], adhesion peptides [19], acrylate groups [20], and other polymers [21]. Alginate hydrogels with modified chains that allow for photocrosslinking has received attention for various applications [22–24]. Solutions containing cells or bioactive molecules can delivered and crosslinking in physiological conditions following exposure to ultraviolet light in the presence of photoinitiators [25]. While there has been success in introducing acrylate groups to allow for photo polymerization, the studies have primarily investigated using large hydrogel structures as scaffolds often with only a single crosslinking mechanism. Very little research has been conducted on the formation of spherical alginate microbeads with dual crosslink systems. Spherical structures are primarily used for islet encapsulation due to the importance of uniform transport and low surface area to volume ratio.

In this paper, a technique for preparing alginate microbeads using both ionic and covalent crosslinks is described. Alginate was modified by functionalizing carboxylate moieties with 2-aminoethyl methacrylate hydrochloride (AEMA), allowing for covalent attachment between the alginate chains [26]. The effect on AEMA-modification was investigated to determine which conditions allowed the alginate to form spherical gels first through ionic crosslinking followed by photocrosslinking. The methacrylation efficiency was varied and *in vitro* studies of mechanical stability, long term swelling, and cell viability were performed. To determine the stability of methacrylated alginate microbeads *in vivo*, a modification of a current omentum pouch animal model was utilized [27]. Lipopolysaccharide (LPS) was injected locally onto the omentum during implantation of microbeads to induce increased inflammation as a challenge to the implanted microbeads.

2. Methods

2.1. Materials

Sodium Alginate (viscosity = 20–40 mPa s), 2-hydroxy-2-methylpropiophenone (Irgacure 1173), 2-morpholinoethane-sulfonice acid (MES), N-hydroxysuccinimide (NHS), 1-ethyl-3-(3-dimethylaminopropyl)-carbodiimide hydrochloride (EDC), lipopolysaccharide (LPS) from *Escherichia coli* 0111:B4, Dulbecco's Modified Eagle's medium (DMEM), Dulbecco's phosphate-buffered saline (DPBS), and 2-mercaptoethanol were purchased from Sigma-Aldrich (St. Louis, MO). Fetal Bovine Serum (FBS) and penicillin-streptomycin was purchased from Life Technologies (Waltham, MA). MIN6 cell line was purchased from AddexBio (San Diego, CA). 2-Aminoethyl methacrylate hydrochloride (AEMA) was purchased from Polysciences (Warminster, PA). Live-Dead kit was purchased from Invitrogen (Eugene, OR). Solutions for alginate microbead fabrications were made using the following chemicals: HEPES, NaCl, $MgCl_2$ (Fisher Scientific); $CaCl_2$ (Acros).

2.2. Synthesis and characterization of methacrylated alginate

Methacrylated alginate was synthesized based on the modification of a previous protocol developed by Jeon et al. (Fig. 1) [28]. Briefly, sodium alginate was dissolved in a buffer solution (1% w/v) consisting of 0.5 M NaCl and 50 mM MES. NHS and EDC were added to the mixture sequentially and mixed for 5 min. AEMA was added to the mixture and the reaction maintained at room temperature for 24 h. The amount of AEMA added to the mixture was varied from 47.5 to 237.5 mg with EDC and NHS concentrations used at levels that maintained a molar ratio of NHS:EDC:AEMA equal to 1:2:1. After 24 h, the reaction was precipitated with excess acetone using a Buchner funnel through 5 μm filter paper. The product was recovered and dissolved in 50 mL of deionized (DI) water and precipitated again with acetone. The product was dissolved in 50 mL DI water and dialyzed (MWCO 3500) against DI water for 3 days. The methacrylated alginate solution was filtered with a 0.22 μm filter and lyophilized. Control, unmodified alginate was processed in the same manner in the absence of AEMA.

^{1}H nuclear magnetic resonance (NMR) was performed to evaluate methacrylation. Methacrylated alginate (15 mg) was dissolved in 1 mL of deuterium oxide and placed in NMR tubes. The NMR spectrum of the methacrylated alginate was recorded on a Bruker 300 Ultrashield NMR spectrometer. The methacrylation efficiency was calculated for all groups. The methacrylation efficiency (ME) was determined as the ratio of the integrals for the methylene protons of methacrylate (δ5.3–5.8 ppm) to alginate protons (δ3.5–4.0 ppm) [18].

FTIR spectra were recorded on a FTIR spectrometer (Nicolet iS 10 FT-IR Spectrometer, Thermo, USA) equipped with a Smart iTX Accessory with a germanium crystal. An average of 120 scans for each sample. Air was used as a background before each scan. Baseline correction was performed using OMNIC spectral analysis software.

2.3. Fabrication of alginate microbeads

Microbeads were prepared using a standard method of injection into a cationic crosslinking solution [5,29]. Methacrylated alginate was dissolved in alginate solution consisting of 25 mM HEPES, 118 mM NaCl, 5.6 mM KCl, 2.5 mM $MgCl_2$. The dissolved precursor was extruded through a 1 mL syringe with a blunt 25-gauge needle into 15 mL crosslinking solution bath. The crosslinking solution consisted of 100 mM $CaCl_2$, 10 mM HEPES, and 0.05% (w/v) Irgacure 1173 (photoinitiator). The beads were incubated in the crosslinking solution and exposed to UV light for 15 min. After 15 min the beads were washed twice with normal saline (0.9% NaCl). A schematic of the bead synthesis steps is shown in Fig. 2. The concentration of alginate was varied between 1.5 and 2.0%. Images of beads (n = 10) were taken to assess bead diameter and perimeter. The measurements were used to calculate the shape factor for the beads using the ratio of the radius obtained from the area over the radius obtained from the perimeter, $R_{area}/R_{perimeter}$. A shape factor of one signifies a perfect circle and less than one denotes a more irregular shape.

Scanning electron microscopy (SEM) was used to evaluate the surfaces of the microbeads. Alginate microbeads were incubated in 2.5% glutaraldehyde at 4 ° C for 2 h. The

microbeads were washed 3 times with distilled water. Microtubes containing the microbeads and distilled water were frozen in liquid nitrogen and then lyophilized overnight. Randomly selected microbeads were deposited on carbon conductive tape adhered to SEM aluminum stubs. The beads were analyzed using a Phenom PRO Desktop SEM (Phenom-World, Netherlands) operated at 10 kV.

2.4. Stability and swelling *in vitro*

To assess the stability of alginate beads *in vitro*, a shaker flask test was utilized [30]. Alginate beads were prepared as described above. Fifty alginate beads were placed in 50 mL of normal saline in an Erlenmeyer flask. The flask was placed on a stir plate set to 125 rpm for 18 h. After 18 h, the beads were collected over a 100 μm cell strainer and counted.

To determine long term swelling properties [4], microbeads were incubated in three different solutions in a 37 ° C humidified atmosphere over a period of 150 days. Fresh alginate beads were prepared and incubated in three different incubation media: 1) saline, 2) saline with 22 mM $CaCl_2$, and 3) saline with 2 mM $CaCl_2$. These conditions were used to evaluate the influence of calcium concentration on bead stability [4]. Images of microbeads (n = 5) were taken and bead diameter quantified. The media was replaced after the beads were imaged.

2.5. Mesh size and permeability

Polymer mesh size in the microbeads was calculated from swelling studies using an approach described previously by Lee et al. [31]. Twenty-five microbeads were weighed in the swollen state and then dried in a vacuum oven over night. Following incubation, the mass of the dried beads was determined, and the volume fraction of microbeads calculated using the following equation:

$$v_2 = \left[m_{dry}/\rho_{alginate}\right]/\left[(m_{dry}/\rho_{alginate}) - ((m_{wet} - m_{dry})/\rho_{water})\right],$$

where m_{dry} is the weight of the dried microbeads, m_{wet} is the weight of the swollen microbeads, ρ_{water} is the density of water (1 g/cm^3) and $\rho_{alginate}$ is the density of the alginate (1.6 g/cm^3). The crosslink density n (mol/cm^3) was calculated from the Flory-Rehner Equation:

$$n = -\left[ln(1 - v_2) + v_2 + \chi_1 v_2^2]/[V_1(v_2^{1/3} - 0.5v_2)\right],$$

where χ_1 is the Flory-Huggins interaction parameter (0.5), and V_1 is the molar volume of water (18 cm^3). The molecular weight between crosslinks (g/mol) is given by: $M_c = \rho_P = n$.

The mesh size, ζ was then approximated by: $\xi = v_2^{-1/3} l * (2M_c/M_r)^{1/2} C_n^{1/2}$, where M_r is the molecular weight (390.1 g/mol) of the repeat unit, l is the carbon-carbon bond length of monomer unit (5.15 Å), and C_n is the characteristic ratio for alginate (21.1).

The permeability of dual crosslinked alginate microbeads was examined by incubation of individual beads in 250 μl of 2 mM $CaCl_2$ solution with 10 μl FITC-BSA (r_s = 3.6 nm) at a

concentration of 5 mg/ml. Confocal images of the beads were taken at 30 min, 5 h, 1 day, and 3 days. All images were obtained using a confocal laser scanning microscope with a low pass filter at 505 nm and excitation at 488 nm. One bead was picked as a representative for that specific group and intensity profiles were obtained using ImageJ software and plotted using MATLAB.

2.6. Cell viability and function

MIN6 cells (AddexBio) were encapsulated within beads to evaluate toxicity of the crosslinked alginate. 1×10^6 cells per 1 mL of the alginate precursor solution were mixed to obtain an alginate solution containing cells. The alginate and cell mixture was extruded through a 25-gauge needle into a crosslinking solution containing Irgacure 1173 (photoinitiator). The beads were exposed to UV light for 15 min to allow covalent crosslinking. After 15 min the beads were washed twice with saline and cultured in DMEM containing 15% FBS, 1% antibiotic/antimycotic, and 0.05 mM 2-mercaptoethanol in a humidified incubator at 37 ° C with 5% CO_2. Every two days, the media was changed. At days 1, 4, 7, and 10, the beads were washed twice with 1xDPBS and incubated in Live/Dead media for thirty minutes. Fluorescence images (Carl Zeiss AG, Germany) were taken of live (488 nm excitation, 505–530 nm bandpass filter, green) and dead cells (543 nm excitation, 560 nm longpass filter, red) with a 5 × objective and the number of live cells quantified. Formulations tested was for concentrations of 1.5%, 1.8%, and 2.0% (w/v) for control, 0.31%, 1.12%, 2.19%, and 3.9% ME alginate.

The media used for insulin secretion was Krebs Ringer bicarbonate solution, pH 7.2. Briefly, three different formulation of alginate microbeads were synthesized as described above at a concentration of 5×10^6 cells per 1 mL of alginate precursor. The groups were control alginate, 1.12 MethAlg, and 3.95 MethAlg all at 1.5%. The microbeads were cultured for 3 days in DMEM containing 25 mM Glucose. After 3 days, the microbeads were subsequently washed in Krebs Ringer bicarbonate solution (2 mM glucose) and incubated for two hours at 37 ° C with 5% CO_2. Media was then replaced with Krebs Ringer containing 20 mM of glucose for two hours with 20 μl of media collected every 20 min. Insulin was measured by ELISA (Crystal Chem, Downers Grove, IL, USA).

2.7. *In vivo* stability model

Animal experiments were carried out using procedures approved by Chang Gung Hospital or Illinois Institute of Technology's Institutional Animal Care and Use Committee. An omentum pouch model [27] was used to evaluate microbeads *in vivo*. Two alginate conditions were examined: control ionic-crosslinked alginate microspheres and dual crosslinked alginate microspheres (1.12 MethAlg) both at 1.5% concentration. A total of 16 animals were used, 4 per group per time point (1 and 3 weeks). Male Sprague Dawley rats (300–400 g, n = 4; Taiwan) were anesthetized initially with 5% isoflurane. Body temperature was maintained at 37 ° C with a heating pad, and anesthesia was maintained with a 2% isoflurane/oxygen gas mixture during the procedure. Each animal had their abdomen shaved, and skin scrubbed with isopropyl alcohol followed by a povidoneiodine antiseptic solution. The omentum was surgically exposed by midline laparotomy. First, the skin was separated from muscle and a ~2 inch incision was made. Next, the underlying

muscle was cut to expose the organs and the greater omentum was carefully pulled from the abdomen. Using 4-0 Ethilon suture, a purse-string suture was positioned around the edges of the omentum to create a pouch for the beads. Fifty alginate beads were placed on the anterior surface of the exposed omentum. LPS (100 μl of 50 μg LPS dissolved in 1 mL saline) was directly injected onto the anterior surface of the omentum. Afterwards, the pouch was folded over and sutured to secure the beads inside. The underlying muscle and then skin were closed with 4-0 Ethilon suture. After surgery, the animals were allowed to recover and monitored closely.

At each time point (week 1 and week 3) the omenta were explanted, fixed in formalin, and prepared for histological characterization and imaging. The tissues were processed for histology using standard methods and tissues were paraffin embedded. Samples were sectioned at 5 μm thickness and stained with hematoxylin and eosin (H&E) and Massons Trichrome. Tissue sections were imaged using an Axiovert 200 inverted microscope (Carl Zeiss MicroImaging).

2.8. Microbead size and stability

To evaluate the influence of microbead size on the impact of dual crosslinking, shaker flask tests were performed as described in Section 2.4 on microbeads fabricated with a two-channel air jacket microencapsulator (air jacket 15 psi and alginate jacket pressure of 10 psi). A 25-gauge needle was used to create microbe-ads with a mean diameter of 1344 μm ± 45 μm.

The *in vivo* stability tests described above were performed on the smaller microbeads synthesized with two-channel air jacket microencapsulator. Two alginate conditions were examined: control ionic-crosslinked microspheres and dual crosslinked micro-spheres 1.12 MethAlg both at 1.5% w/v concentrations. Microbeads were autoclaved at 110° for 20 min in 0.9% saline solution supplemented with 2 mM $CaCl_2$ to sterilized the beads. Male Sprague Dawley rats (300–400 g, n = 2; Envigo) were anesthetized initially with 5% isoflurane. Body temperature was maintained at 37 ° C with a heating pad, and anesthesia was maintained with a 2% isoflurane/oxygen gas mixture during the procedure. The surgical procedure was performed as described above. At 1 week time the omenta were explanted, fixed in formalin, and prepared for histological characterization and imaging.

2.9. Statistical analysis

Statistical analysis was performed using GraphPad Prism. All statistical data are expressed as mean ± standard deviation. *In vitro* data were analyzed using one-way ANOVA with a Tukey's post test for normally distributed data. Values of $p < .05$ were considered statistically significant.

3. Results

3.1. Methacrylation efficiency

Methacrylated alginate was produced by reacting alginate (500 mg) with AEMA. Changes in the AEMA:alginate ratio resulted in varying methacrylation efficiency. ^{1}H NMR of

alginate and methacrylated alginate was used to evaluate the product (Fig. 3G). From NMR data, peaks for the methylene (δ5.3–5.8 ppm), methyl (δ1.8), and alginate (δ3.5–4 ppm) were observed on the spectra. Lower degrees of methacrylation, had smaller value for area under the curves with some shift in the spectra. The ME increased with increasing AEMA, with 0.31% ± 0.11, 1.12% ± 0.14, 2.19% ± 0.54, 3.95% ± 0.35, and 5.55% ± 0.50 efficiency for 47.5 mg, 95 mg, 142.5 mg, 190 mg, and 237.5 mg AEMA, respectively. Acrylation results from modification of carboxyl groups in alginate that are also required for ionic crosslinking. Beads were formed using a standard ionic crosslinking mechanism to identify the ME limit at which bead formation was disrupted (Fig. 3). Spherical beads were formed with up to 190 mg of AEMA (19:50 AEMA:Alginate). Higher amounts of AEMA resulted in gel formation but the bead structure was altered (Fig. 3F). The shape factor, for groups that did form a spherical shape, was greater than 0.85. FTIR spectra further validated the modification of alginate with AEMA groups, Supplemental Fig. S1. The alginate samples exhibited a shift and broadening of the (1600 cm^{-1}) peak after coupling with AEMA. The new center of the peak is 1603 cm^{-1} (FS1.B and FS1.C) as a result of the amide I bond between 1620 and 1640 cm^{-1}. In addition, a visible shoulder peak centered at 1542 cm^{-1} was observed for the amide II bond. SEM was used to examine the surface of control and dual cross-linked microbeads. Qualitatively, there were no differences in the surfaces of the beads, FS2.

3.2. Microbead stability *in vitro*

The stability of methacrylated alginate microbeads was assessed first *in vitro* with a shaker flask assay. Fifty alginate microbeads were placed in 50 mL 0.9% NaCl solution and placed on a stir plate set at 125 rpm at room temperature. After 18 h, the beads were counted. Under these conditions, all ionic cross-linked alginate microbeads were broken down regardless of alginate concentration (1.5%, 1.8%, and 2.0%). However, the dual crosslinked microbeads exhibited increased integrity compared with control without any breakdown even at the lowest ME (0.31% Fig. 4).

The time-dependent swelling of alginate microbeads was evaluated under various calcium conditions (0, 2, and 22 mM $CaCl_2$). Calcium concentration influences the rate of breakdown of alginate microbeads with concentrations typical of physiological levels providing outcomes that reproduce *in vivo* degradation via an ion substitution [4]. Fig. 5 shows the swelling characteristics of methacrylated alginate beads in saline solution with 0 mM $CaCl_2$. Ionic-crosslinked alginate microbeads exhibit significant swelling within one day followed by complete failure within two days, regardless of alginate concentration. Covalent crosslinking substantially increased stability in culture. The 0.31% ME groups exhibited significant swelling for all concentrations compared with other methacrylation levels. The microbeads for the 0.31% ME took 63, 105, and 151 days to break down for the 1.5%, 1.8%, and 2.0% concentrations. All remaining groups remained in saline and exhibited very little swelling as seen from Fig. 5. Microbeads incubated in 2 mM and 22 mM $CaCl_2$ still remained in solution up to 150 days with varying degrees of swelling including groups without covalent crosslinking due to the presence of calcium ions in the incubation media.

3.3. Mesh size and permeability

Mesh size, molecular weight between crosslinks and crosslink density were calculated based on microbead swelling experiments. The crosslink density of the polymer chains increased and the molecular weight between crosslinks decreased with increasing methacrylation (Fig. S3B). Consistent with these results, the mesh size decreased with both higher methacrylation efficiency and increased alginate concentrations (Fig. 6). The mesh size varied between 67 and 96 nm for all conditions.

Permeability of the microbeads was examined experimentally to provide insight into if the increased crosslinked density/decreased mesh size dramatically alters transport. The microbeads were incubated with FITC-BSA and intensity profiles obtained at various time points (Fig. 7). By 5 h FITC-BSA could be observed within the core of all groups (Alg, 1.12 MethAlg, 3.95 MethAlg). Control alginate appeared to allow more rapid diffusion of the protein into the core. At 5 h, the center of the microbeads had nearly 40% of the intensity of FITC-BSA in the incubation media for the 2% concentration. When compared with 1.12 MethAlg and 3.95 MethAlg these values were at 11% and 5%, respectively. By day 3 all groups had similar levels of FITC-BSA in the core relative to the incubation media.

3.4. Cell viability

MIN6 cells were encapsulated in alginate microbeads and cell viability examined by fluorescence staining using a commercially available cell assay (Fig. 8). Twenty-four hours after formation, the majority of the cells were alive and a few dead cells were observed within the microbeads under all crosslinking conditions. Further culture of microbeads showed live cells up to day 10. The total number of cells appeared to be lower by day 10 for all conditions, but the percentage of dead cells was low. Quantitative analysis of cell viability showed greater than ~95% viability for all groups at all time points (Fig. 9).

Insulin secretion of MIN6 cells encapsulated within Alg, 1.12 MethAlg, and 3.95 MethAlg at 1.5% is shown in Fig. 10. The cells displayed increased in insulin secretion when stimulated with 20 mM glucose. There was a four-fold increase in insulin secretion ($p \leq .05$) for Alg, 1.12 MethAlg, and 3.95 MethAlg between time 0 and 100 min. The baseline level of insulin secretion was higher for the Alg 1.12 group compared with the modified group however the data was not statistically significant between the groups.

3.5. *In vivo* stability model

Two different alginate conditions, Alg 1.5% (w/v unmodified alginate) and 1.12 MethAlg 1.5% (w/v 1.12% ME alginate), were evaluated in a rat omental pouch model. The MethAlg conditions were selected as the level where spherical beads were formed and showed increase stability testing *in vitro* with viable cells following encapsulation. During microbead implantation 5 μg LPS was injected to stimulate a robust inflammatory response in order to challenge that stability of the alginate microbeads. Preliminary studies determined that at this level LPS was able to result in levels of inflammation that have been shown to result in microbead breakdown in other models [27] without signs of systemic toxicity.

At weeks 1 and 3, the microbeads were harvested (Fig. 11) and processed for histological analysis. During harvest, it was observed that there was significant inflammation at week 1 with breakdown of the ionic crosslinked alginate microbeads (Fig. 11A), whereas the dual crosslinked microbeads were still intact (Fig. 11B). By week 3, both groups exhibited decreased inflammation and the dual cross-linked microbeads remained stable (Fig. 11D).

Hematoxylin and eosin and Masson's trichome stains were performed on the samples harvested at 1 and 3 weeks to evaluate microbead structure and inflammatory response. The dual cross-linked alginate microbeads were seen within the tissue even in the presence of a robust inflammatory response at week 1 (Fig. 12C, D). Bead fragments were observed within the omenta containing ionically crosslinked alginate microbeads (Fig. 12A, E). The fragments were encapsulated by fibrotic tissue with multinucleated foreign body giant cells observed near the biomaterial surface. Mason's Trichrome stains further confirmed the robust inflammatory response seen by week 1 in both groups due to the LPS (Fig. 13). However, at 3 weeks a high level of inflammation was maintained around ionic crosslinked microbeads particularly around the alginate fragments with very little collagen deposition (Fig. 13F). However, samples with dual crosslinked alginate microbeads had less inflammation with collagen deposition near the surface of the microbeads, suggesting progression to granulation tissue and encapsulation of the implants (Fig. 13H).

3.6. Effect of bead size on stability

Dual crosslinking with methacrylated alginate also resulted in improved stability for smaller (~1300 μm) microbeads formed with an encapsulator system. Ionic crosslinked groups broke down rapidly in *in vitro* stability tests independent of concentration. Unlike larger beads used in the previous studies *in vitro* breakdown was observed at the lowest ME (0.31%) (Fig. 14A). However, at higher ME the beads exhibit 100% stability in the shaker flask test.

Two different alginate conditions, Alg 1.5% (w/v unmodified alginate) and 1.12 MethAlg 1.5% (w/v 1.12% ME alginate), were evaluated in a rat omental pouch model. Similar to the larger microbeads, 1.12 MethAlg microbeads remain intact after exposure to LPS at 1 week (Fig. 14C). Individual alginate microbeads are observed with inflammatory tissue surrounding the surface of the microbeads. The ionically crosslinked group had complete breakdown of microbeads with small fragments surrounded by dense inflammatory tissue (Fig. 14B).

4. Discussion

In this research, alginate microbeads with both ionic and covalent crosslinks were developed as a method to increase microbead stability. Alginate was modified with AEMA to introduce methacrylate side chains that enabled the introduction of covalent crosslinks via photo crosslinking. Improvement in alginate microbead stability could address a challenge of current encapsulation processes where implanted materials break down following implantation resulting in loss of functional cells. The results of this study demonstrate that dual crosslinking of alginate results in increased stability.

Alginate microbeads have been investigated extensively for cell encapsulation. However, there are concerns in regards to the stability of implanted alginate microbeads. Literature results vary but it is clear in both clinical and pre-clinical studies that there is a subset of patients where the graft fails and evidence suggests that breakdown of the alginate can be a factor [12]. The mechanisms that lead to alginate breakdown are not fully established due, in part, to inconsistent data in pre-clinical models. Transplantation site, graft biocompatibility, and properties of the alginate microbe-ads may all contribute to overall success of the system [32]. These factors can be interdependent, as the biomaterial properties can drive the local inflammatory response which, in turn, leads to failure of the system [33]. In addition, microbead breakdown may exacerbate the inflammatory response leading to complete failure. Stabilizing the alginate microbeads may prevent breakdown, allowing the local inflammatory response to resolve, circumventing further complications.

Several attempts have been made to produce alginate microbe-ads with improved mechanical stability to overcome the observed failure in clinical applications. One method is incorporation of poly (ethylene glycol) (PEG) with alginate chains. Covalent crosslinking of PEG with alginate was accomplished by linking phosphine-terminated PEG to azide-functionalized alginate through Staudinger ligation, followed by ionotropic gelation of the alginate using barium ions. The dual crosslinked alginate-PEG microspheres were less prone to swelling and exhibited increased stability upon exposure to chelating agents than alginate spheres alone [9,34]. An alternative to crosslinking with PEG involves direct introduction of crosslinking through photoactivatable groups, as performed in these studies. Spheres with increased mechanical stability have been obtained by linking methacrylate groups and N-5-azido-2-n itrobenzoylsuccinimide to the alginate molecule, as well as with the addition of acrylate and *N*-vinylpyrrolidone into the calcium bath [35–37]. The concept of increasing mechanical stability of alginate microbeads as a means to increase long-term success of alginate cell encapsulation systems has been extensively tested *in vitro*. However, none of these studies addressed stability *in vivo*. Pre-clinical animal studies are required to advance these findings to the clinical testing stage.

The difference between this method and previous methods is both the degree of methacrylation studied and the use of the alginate for microbead applications. The lower level of methacrylation allows the carboxylic acid groups to interact with divalent cations to form that ionic interactions that provide the initial microbead shape. These unmodified chains could also be targeted for introduction of cell adhesion peptides for enhanced cell function. While the other methods have been investigated for increasing stability, to our knowledge, increased stability has not been shown with these systems. In this work, we have been able to successfully increase the stability *in vitro* but also showed the integrity of microbeads *in vivo* under the presence of a robust inflammatory response induced by LPS in a small animal model.

In this work alginate microbeads were stabilized via attachment of AEMA to the alginate chains. The attached AEMA groups form covalent crosslinks via a free radical process. The degree of methacrylation was proportional to AEMA:alginate ratio utilized in the reaction (Fig. 3). Interestingly, a threshold existed for the amount of AEMA included, beyond the beads could not gel via the initial ionic crosslinking step. In ionic crosslinking the negatively

charged carboxylate group interact with the divalent cations allowing the initial spherical shape to be maintained following injection into the crosslinking solution. With high methacrylation efficiencies, an insufficient amount of free carboxylate groups were available for bead formation. Stability testing of alginate microbe-ads showed that unlike ionic crosslinked microbeads, dual cross-linked alginate microbeads remained intact regardless of modification level. Long term swelling of microbeads in static incubation presented to be more complex. Unmodified alginate microbeads broke down within two days for 1.5%, 1.8%, and 2.0% concentrations. One group of methacrylated alginate microbeads, the 0.31 MethAlg 2.0%, remained in solution for 151 days. The group exhibited osmotic swelling to three times the initial size and subsequently dissolved. The likely reason for long term swelling is the slow hydrolysis of the ester linkages of the AEMA groups, which promotes dissolution of alginate microbeads. This was not observed with other methacrylated alginate microbeads likely due to the higher ME. Alginate microbeads with higher ME exhibited very minimal swelling, no appreciable change in size, and remained intact after 150 days.

All conditions exhibited >95% cell viability following encapsulation. However, the total number of cells appeared to decrease from day 1 to day 10. Several aspects of the synthesis of chemically modified alginate microbeads has the potential to negatively affect cell viability, including the encapsulation process, the exposure to free radicals during crosslinking, and the presence of AEMA. One possible reason for this observed cell loss is due to the properties of alginate, being a relatively inert material that does not support cell adhesion [26]. Alternatively, the density of encapsulated insulinoma cells may not be high enough to allow intercellular interactions and release of trophic factors that promote survival and proliferation [38]. The purpose of the assay was to determine if the encapsulation processes, the exposure to free radicals, or the AEMA had any immediate effect on cell viability, which was not observed. Insulin secretion assay showed the MIN6 cells exhibited glucose response regardless of alginate conditions. Future studies will address the alginate and cell conditions optimal for functional outcomes.

The *in vivo* stability of alginate microbeads was tested by implanting fifty beads into the omentum of non-diabetic rats. When implanted in this way, microbeads can easily be retrieved for post-transplant analysis. In the absence of a sustained inflammatory challenge, we have previously shown unmodified beads remain intact when implanted into the omentum [39]. However, many pre-clinical studies have shown that some implantation conditions can result in increased inflammation and bead failure [27]. It is not clear if this is due to alginate composition, shape, size [15] or surgical conditions. In addition, many crude alginates contain components that can elicit inflammatory responses, including endotoxins [40,41]. In this study, we developed a method that introduced an increased inflammatory challenge to the microbeads following implantation. Lipopolysaccharide (LPS) was applied directly onto the omentum at the time of implantation to promote inflammation. The local application of LPS provides a method for controlling the inflammatory challenge regardless of alginate conditions that serves as a test the stability of alginate systems.

The integrity of modified and non-modified microbeads was evaluated one and three weeks post-implantation. After 1 week, the unmodified alginate microbeads exhibited complete breakdown, as demonstrated in the representative histological images. By comparison, dual

crosslinked modified (1.12 MethAlg 1.5%) microbeads remained intact (Figs. 12C, D and 13C, D). Breakdown of unmodified microbeads persisted through three weeks (Figs. 12E, F and 13E, F), and modified microbeads remained intact through the same period (Figs. 12G, H and 13G, H). Inflammatory tissue surrounds the remaining fragments of broken down alginate beads and includes foreign body giant cells. Masson's trichrome staining reveals a thin layer of collagen surrounding the intact beads (Fig. 13H). The overall inflammatory tissue appears to be qualitatively less for modified microbeads compared with unmodified alginate microbeads suggesting that as beads break down inflammation is increased.

It is likely that the implantation of crude alginate microspheres, along with the exogenous LPS challenge, initiates an acute inflammatory response which includes arrival of neutrophils to the implant site, activation of macrophages, degranulation of mast cells, and release of pro-inflammatory mediators [14]. We hypothesize that unmodified alginate microbeads undergo initial breakdown due to acute inflammation by week 1 (Fig. 12A, B), and that the increased stability of the crosslinked alginate prevents this microbead fragmentation (Fig. 12C, D). The breakdown of control microbeads may further exacerbate the local inflammatory response to a more persistent state of inflammation as observed by Week 3 in the case of unmodified microbeads. This is supported by previous studies demonstrating that implantation of large (>1500 μm) microbeads composed of a variety of different biocompatible materials elicited attenuated foreign body reactions as compared to smaller (<500 μm) microbeads [15]. In our study, the mean diameter of microbeads used was 2362 μm and 2560 μm, respectively for unmodified and modified groups. Once they begin to break apart (by week 1), the smaller fragments may exacerbate inflammation to a chronic state due to their size. By week 3, these smaller fragments of alginate microbeads promote an upregulation of inflammatory tissue and infiltration of mononuclear cells. The covalent crosslinking of modified alginate microbeads prevents the initial break down, circumventing chronic inflammation. The tissue surrounding these methacrylated alginate microbeads is a normal healing response where a layer of collagen surrounds the implant (Fig. 9H) and promotes neovascularization [33]. Similar observations were seen when smaller beads (~1350 μm) were implanted into the omenta with LPS. The ionically cross-linked microbeads had complete failure whereas the dual cross-linked, 1.12 MethAlg 1.5% had intact microbeads (Fig. 14). These studies show that the dual crosslinking could be used to enhance the stability of microbeads formulated at different sizes. However, the optimal conditions may vary with bead size and alginate composition. Future studies will characterize the phenotype of macrophages and other immune cells during the observed chronic inflammation in the presence of modified and unmodified alginate microbeads. Our data here suggest that mononuclear cells present at the implant site surrounding modified alginate microbeads may promote an anti-inflammatory, pro-healing phenotype. This can be confirmed by the presence of IL-10, TGF-β, and $CD163^{+}$ [42].

5. Conclusion

Alginate microbeads have been investigated for several therapeutic interventions including cell delivery and cell encapsulation. In the context of current protocols, implantation of alginate microbeads can fail due to the inflammatory response or mechanical stresses. In this study microbeads were fabricated from methacrylated alginate which allowed for covalent

crosslinking in addition to ionic interactions with divalent cations. Microbeads were tested *in vivo* using an omentum pouch model with local LPS injection. Methacrylated alginate microbeads were stable under an inflammatory challenge. Covalent crosslinking may be an important addition to cell encapsulation protocols to enhance long-term survival and function.

Supplementary Material

Refer to Web version on PubMed Central for supplementary material.

Acknowledgments

This work was supported, in part, by funding from the National Institutes of Health (grants 5R01EB020604), the National Science Foundation (CBET-1263994, IIS-1125412, 1614365, EEC-1461215), the Department of Veterans Affairs (5 I01 BX000418-06, 1 IK2 RX002305-01A2), Chang Gung Memorial Hospital (CMRPG3C1062), and the Ministry of Science and Technology (MOST).

References

1. Khanna O, Huang JJ, Moya ML, Wu CW, Cheng MH, Opara EC, Brey EM. FGF-1 delivery from multilayer alginate microbeads stimulates a rapid and persistent increase in vascular density. Microvasc Res. 2013; 90:23–29. [PubMed: 23978335]
2. Schneider S, Feilen PJ, Brunnenmeier F, Minnemann T, Zimmermann H, Zimmermann U, Weber MM. Long-term graft function of adult rat and human islets encapsulated in novel alginate-based microcapsules after transplantation in immunocompetent diabetic mice. Diabetes. 2005; 54(3):687–693. [PubMed: 15734844]
3. Rowley JA, Madlambayan G, Mooney DJ. Alginate hydrogels as synthetic extracellular matrix materials. Biomaterials. 1999; 20(1):45–53. [PubMed: 9916770]
4. Moya ML, Morley M, Khanna O, Opara EC, Brey EM. Stability of alginate microbead properties *in vitro*. J Mater Sci Mater Med. 2012; 23(4):903–912. [PubMed: 22350778]
5. Somo, SI., Khanna, O., Brey, EM. Alginate microbeads for cell and protein delivery. In: Opara, EC., editor. Cell Microencapsulation: Methods and Protocols. Springer; New York, NY: 2017. p. 217-224.
6. Zekorn TD, Horcher A, Mellert J, Siebers U, Altug T, Emre A, Hahn HJ, Federlin K. Biocompatibility and immunology in the encapsulation of islets of Langerhans (bioartificial pancreas). Int J Artif Organs. 1996; 19(4):251–257. [PubMed: 8786177]
7. Basta G, Montanucci P, Luca G, Boselli C, Noya G, Barbaro B, Qi M, Kinzer KP, Oberholzer J, Calafiore R. Long-term metabolic and immunological follow-up of nonimmunosuppressed patients with type 1 diabetes treated with microencapsulated islet allografts: four cases. Diabetes Care. 2011; 34(11):2406–2409. [PubMed: 21926290]
8. Qi M, Strand BL, Mørch Y, Lacík I, Wang Y, Salehi P, Barbaro B, Gangemi A, Kuechle J, Romagnoli T, Hansen Ma, Rodriguez La, Benedetti E, Hunkeler D, Skjåk-Braek G, Oberholzer J. Encapsulation of human islets in novel inhomogeneous alginate-ca2+/ba2+ microbeads: in vitro and in vivo function. Artif Cells Blood Substit Immobil Biotechnol. 2008; 36:403–420. [PubMed: 18925451]
9. Rengifo HR, Giraldo JA, Labrada I, Stabler CL. Long-term survival of allograft murine islets coated via covalently stabilized polymers. Adv Healthc Mater. 2014; 3(7):1061–1070. [PubMed: 24497465]
10. Lawandi J, Tao C, Ren B, Williams P, Ling D, Swan MA, Nassif NT, Torpy FR, O'Brien BA, Simpson AM. Reversal of diabetes following transplantation of an insulin-secreting human liver cell line: melligen cells. Mol Ther Methods Clin Dev. 2015; 2:15011. [PubMed: 26029722]
11. Vegas AJ, Veiseh O, Gurtler M, Millman JR, Pagliuca FW, Bader AR, Doloff JC, Li J, Chen M, Olejnik K, Tam HH, Jhunjhunwala S, Langan E, Aresta-Dasilva S, Gandham S, McGarrigle JJ,

Bochenek MA, Hollister-Lock J, Oberholzer J, Greiner DL, Weir GC, Melton DA, Langer R, Anderson DG. Long-term glycemic control using polymer-encapsulated human stem cell-derived beta cells in immune-competent mice. Nat Med. 2016; 22(3):306–311. [PubMed: 26808346]

12. Kollmer M, Appel AA, Somo SI, Brey EM. Long-term function of alginate-encapsulated islets. Tissue Eng Part B Rev. 2015
13. Ponce S, Orive G, Hernandez R, Gascon AR, Pedraz JL, de Haan BJ, Faas MM, Mathieu HJ, de Vos P. Chemistry and the biological response against immunoisolating alginate-polycation capsules of different composition. Biomaterials. 2006; 27(28):4831–4839. [PubMed: 16766026]
14. Anderson J, Rodriguez A, Chang D. Foreign body reaction to biomaterials. Semin Immunol. 2008; 20:86–100. [PubMed: 18162407]
15. Veiseh O, Doloff JC, Ma M, Vegas AJ, Tam HH, Bader AR, Li J, Langan E, Wyckoff J, Loo WS, Jhunjhunwala S, Chiu A, Siebert S, Tang K, Hollister-Lock J, Aresta-Dasilva S, Bochenek M, Mendoza-Elias J, Wang Y, Qi M, Lavin DM, Chen M, Dholakia N, Thakrar R, Lacik I, Weir GC, Oberholzer J, Greiner DL, Langer R, Anderson DG. Size- and shape-dependent foreign body immune response to materials implanted in rodents and non-human primates. Nat Mater. 2015; 14(6):643–651. [PubMed: 25985456]
16. de Vos P, Smedema I, van Goor H, Moes H, van Zanten J, Netters S, de Leij LF, de Haan A, de Haan BJ. Association between macrophage activation and function of micro-encapsulated rat islets. Diabetologia. 2003; 46(5):666–673. [PubMed: 12750768]
17. Dufrane D, Steenberghe M, Goebbels RM, Saliez A, Guiot Y, Gianello P. The influence of implantation site on the biocompatibility and survival of alginate encapsulated pig islets in rats. Biomaterials. 2006; 27(17):3201–3208. [PubMed: 16497373]
18. Bencherif SA, Sands RW, Bhatta D, Arany P, Verbeke CS, Edwards DA, Mooney DJ. Injectable preformed scaffolds with shape-memory properties. Proc Natl Acad Sci USA. 2012; 109(48): 19590–19595. [PubMed: 23150549]
19. Drury JL, Boontheekul T, Mooney DJ. Cellular cross-linking of peptide modified hydrogels. J Biomech Eng. 2005; 127(2):220. [PubMed: 15971699]
20. Mu C, Sakai S, Ijima H, Kawakami K. Preparation of cell-enclosing microcapsules through photopolymerization of methacrylated alginate solution triggered by irradiation with visible light. J Biosci Bioeng. 2010; 109(6):618–621. [PubMed: 20471603]
21. Mahou R, Borcard F, Crivelli V, Montanari E, Passemard S, Noverraz F, Gerber-Lemaire S, Bühler L, Wandrey C. Tuning the properties of hydrogel microspheres by adding chemical cross-linking functionality to sodium alginate. Chem Mater. 2015; 27(12):4380–4389.
22. Chou AI, Akintoye SO, Nicoll SB. Photo-crosslinked alginate hydrogels support enhanced matrix accumulation by nucleus pulposus cells *in vivo*. Osteoarthritis Cartilage. 2009; 17(10):1377–1384. [PubMed: 19427928]
23. Wang L, Shansky J, Borselli C, Mooney D, Vandenburgh H. Design and fabrication of a biodegradable, covalently crosslinked shape-memory alginate scaffold for cell and growth factor delivery. Tissue Eng Part A. 2012; 18(19–20):2000–2007. [PubMed: 22646518]
24. Samorezov JE, Morlock CM, Alsberg E. Dual ionic and photo-crosslinked alginate hydrogels for micropatterned spatial control of material properties and cell behavior. Bioconjugate Chem. 2015; 26(7):1339–1347.
25. Coates EE, Riggin CN, Fisher JP. Photocrosslinked alginate with hyaluronic acid hydrogels as vehicles for mesenchymal stem cell encapsulation and chondrogenesis. J Biomed Mater Res A. 2013; 101(7):1962–1970. [PubMed: 23225791]
26. Jeon O, Powell C, Ahmed SM, Alsberg E. Biodegradable, photocrosslinked alginate hydrogels with independently tailorable physical properties and cell adhesivity. Tissue Eng Part A. 2010; 16(9):2915–2925. [PubMed: 20486798]
27. Ibarra V, Appel AA, Anastasio MA, Opara EC, Brey EM. This paper is a winner in the Undergraduate category for the SFB awards: evaluation of the tissue response to alginate encapsulated islets in an omentum pouch model. J Biomed Mater Res A. 2016; 104(7):1581–1590. [PubMed: 27144389]

28. Jeon O, Bouhadir KH, Mansour JM, Alsberg E. Photocrosslinked alginate hydrogels with tunable biodegradation rates and mechanical properties. Biomaterials. 2009; 30:2724–2734. [PubMed: 19201462]
29. Khanna O, Larson JC, Moya ML, Opara EC, Brey EM. Generation of alginate microspheres for biomedical applications. J Vis Exp. 2012; 66
30. Chandy T, Mooradian DL, Rao GH. Evaluation of modified alginate-chitosan-polyethylene glycol microcapsules for cell encapsulation. Artif Organs. 1999; 23(10):894–903. [PubMed: 10564287]
31. Lee BH, Li B, Guelcher SA. Gel microstructure regulates proliferation and differentiation of MC3T3-E1 cells encapsulated in alginate beads. Acta Biomater. 2012; 8(5):1693–1702. [PubMed: 22306825]
32. de Groot M, Schuurs TA, van Schilfgaarde R. Causes of limited survival of microencapsulated pancreatic islet grafts. J Surg Res. 2004; 121(1):141–150. [PubMed: 15313388]
33. Anderson JM, Rodriguez A, Chang DT. Foreign body reaction to biomaterials. Semin Immunol. 2008; 20(2):86–100. [PubMed: 18162407]
34. Hall KK, Gattas-Asfura KM, Stabler CL. Microencapsulation of islets within alginate/poly(ethylene glycol) gels cross-linked via Staudinger ligation. Acta Biomater. 2011; 7(2):614–624. [PubMed: 20654745]
35. Dusseault J, Leblond FA, Robitaille R, Jourdan G, Tessier J, Menard M, Henley N, Halle JP. Microencapsulation of living cells in semi-permeable membranes with covalently cross-linked layers. Biomaterials. 2005; 26(13):1515–1522. [PubMed: 15522753]
36. Rokstad AM, Donati I, Borgogna M, Oberholzer J, Strand BL, Espevik T, Skjak-Braek G. Cell-compatible covalently reinforced beads obtained from a chemoenzymatically engineered alginate. Biomaterials. 2006; 27(27):4726–4737. [PubMed: 16750563]
37. Wang MS, Childs RF, Chang PL. A novel method to enhance the stability of alginate-poly-L-lysine-alginate microcapsules. J Biomater Sci Polym Ed. 2005; 16(1):91–113. [PubMed: 15796307]
38. Lin CC, Anseth KS. Cell-cell communication mimicry with poly(ethylene glycol) hydrogels for enhancing beta-cell function. Proc Natl Acad Sci USA. 2011; 108(16):6380–6385. [PubMed: 21464290]
39. Moya ML, Lucas S, Francis-Sedlak M, Liu X, Garfinkel MR, Huang JJ, Cheng MH, Opara EC, Brey EM. Sustained delivery of FGF-1 increases vascular density in comparison to bolus administration. Microvasc Res. 2009; 78(2):142–147. [PubMed: 19555698]
40. Zhang WJ, Laue C, Hyder A, Schrezenmeir J. Purity of alginate affects the viability and fibrotic overgrowth of encapsulated porcine islet xenografts. Transplant Proc. 2001; 33(7–8):3517–3519. [PubMed: 11750500]
41. Rokstad, AMa, Lacík, I., de Vos, P., Strand, BL. Advances in biocompatibility and physico-chemical characterization of microspheres for cell encapsulation. Adv Drug Deliv Rev. 2014:111–130. [PubMed: 23876549]
42. Franz S, Rammelt S, Scharnweber D, Simon JC. Immune responses to implants – a review of the implications for the design of immunomodulatory biomaterials. Biomaterials. 2011; 32(28):6692–6709. [PubMed: 21715002]

Appendix A.Supplementary data

Supplementary data associated with this article can be found, in the online version, at https://doi.org/10.1016/j.actbio.2017.10.046.

Statement of Significance

Alginate, a naturally occurring polysaccharide, has been used for cell encapsulation to prevent graft rejection of cell transplants for people with type I diabetes. Although some success has been observed in clinical trials, the lack of reproducibility and failure to reach insulin dependence for longer periods of time indicates the need for improvements in the procedure. A major requirement for the long-term function of alginate encapsulated cells is the mechanical stability of microcapsules. Insufficient mechanical integrity of the capsules can lead to immunological reactions in the recipients. In this work, alginate was modified to allow photoactivatable groups in order to allow formation of covalent crosslinks in addition to ionic crosslinking. The dual crosslinking design prevents capsule breakdown following implantation *in vivo*.

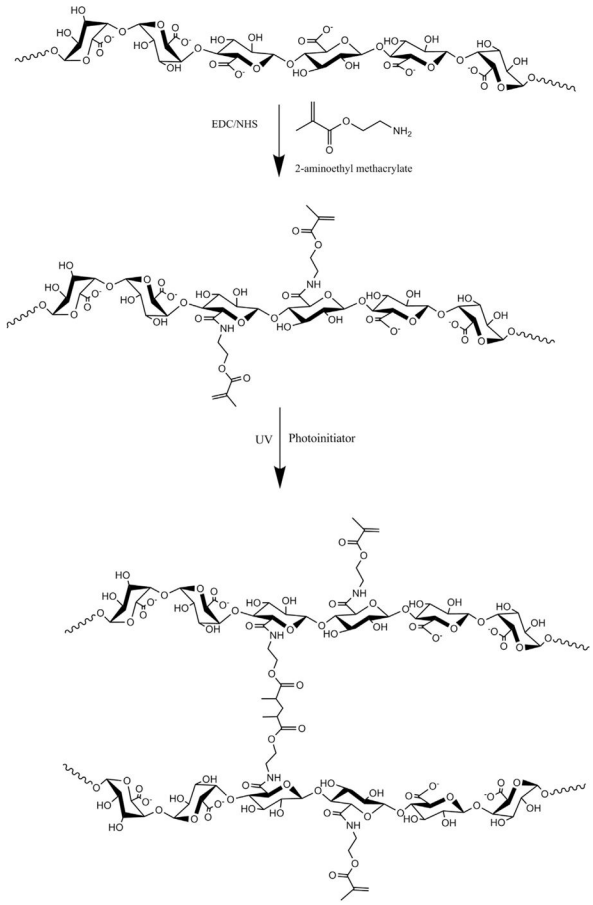

Fig. 1.
Schematic illustration of alginate methacrylation and photocrosslinking of methacrylated alginate.

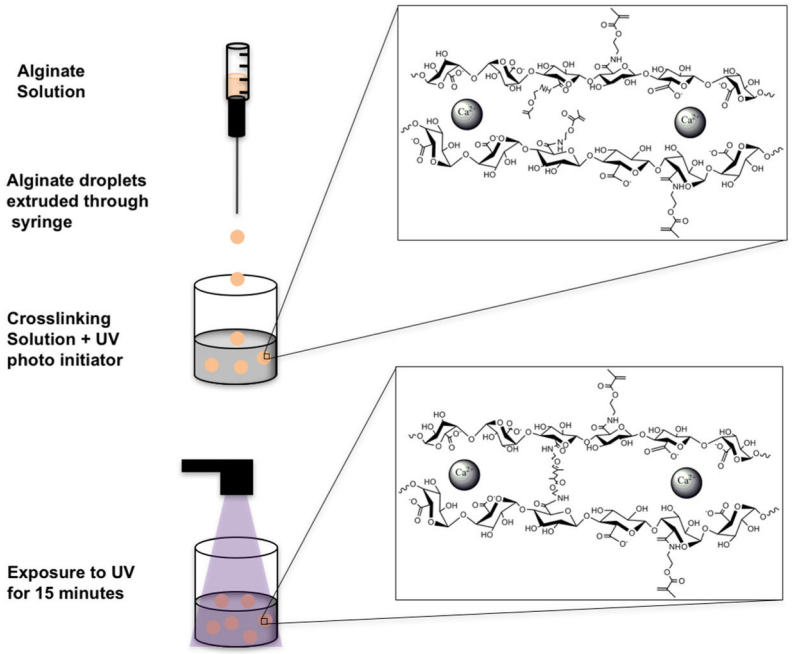

Fig. 2.

Illustration of the procedure for fabrication of alginate microbeads with both ionic and covalent crosslinks. Ionic crosslinks are formed by incubation in a $CaCl_2$ bath followed by exposure to UV to initiate covalent crosslinking.

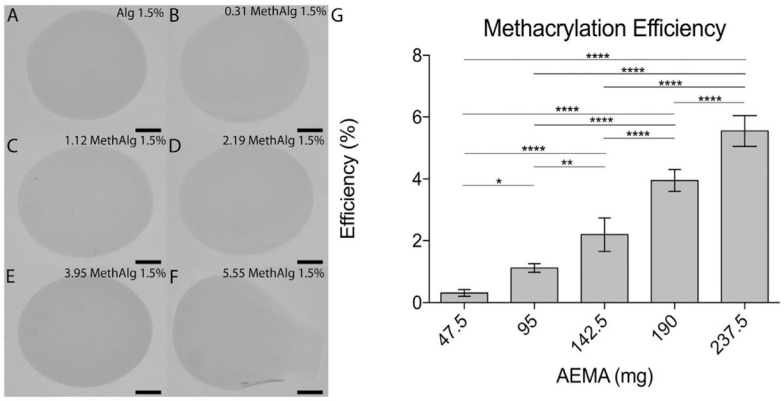

Fig. 3.

Microbead formation depends on methacrylation efficiency which varies with AEMA mass. Alginate microbeads (1.5% w/v) formed from A) 0 (control), B) 47.5, C) 95, D) 142.5, E) 190, and F) 237.5 mg AEMA G) Methacrylation efficiency determined from hNMR plotted versus mass of AEMA. *p ≤.05, **p ≤ .01, ****p ≤ .0001. Scale bar represents 500 μm.

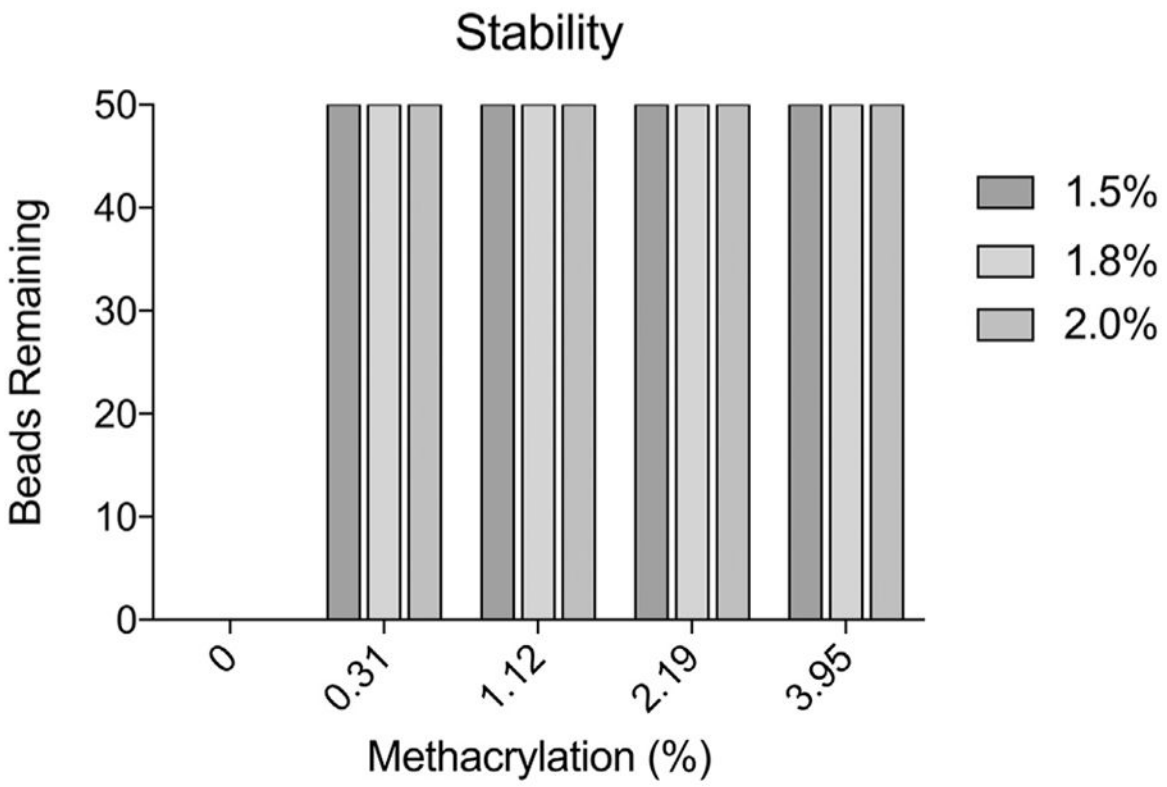

Fig. 4.

Covalent crosslinks increases alginate microbead stability. Number of microbeads remaining, out of 50, following exposure to mechanical forces as a function of methacrylation efficiency and alginate concentration.

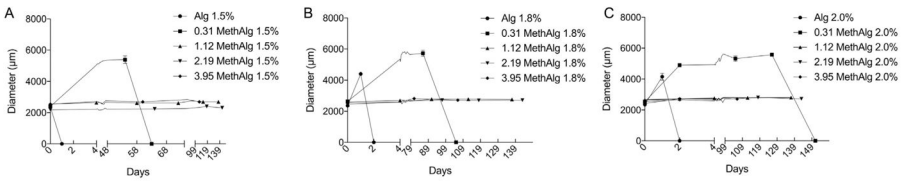

Fig. 5.

Dual crosslinked microbeads maintain their diameter for over 2 months. Diameter versus time for a) 1.5% (w/v), b) 1.8%, and c) 2.0% alginate microbeads in normal saline (0.9% NaCl) at various methacrylation levels.

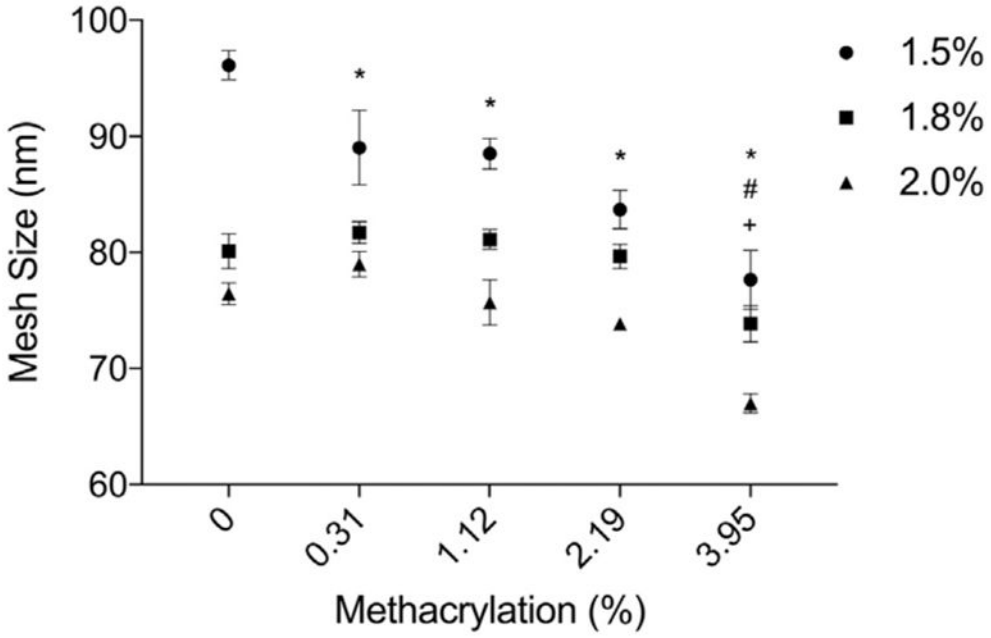

Fig. 6.

Calculated mesh size (ζ) of dual crosslinked alginate microbeads as a function of methacrylation efficiency. Mesh size decreases with increasing concentration of alginate and methacrylation efficiency. $^{*,\#,+}$Denotes statistical significance ($p \leq .05$) between specific group and control for 1.5%, 1.8%, and 2.0% concentrations respectively.

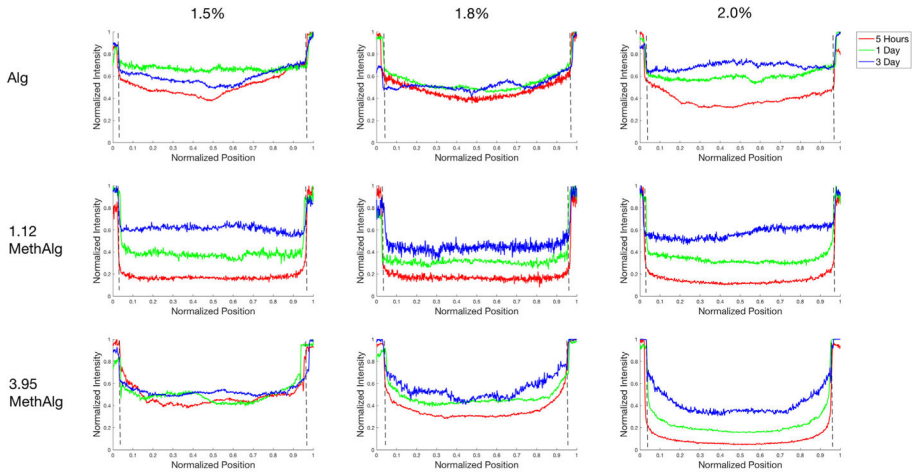

Fig. 7.

Intensity profiles of a cross section of alginate microbeads incubated fluorescently labeled BSA at 5 h, 1 day, and 3 days. The BSA was present within the core of the microbeads at 5 h for all groups with varying levels of intensity. The dashed line represents the margins of the beads. Data from a representative microbead is shown for each condition.

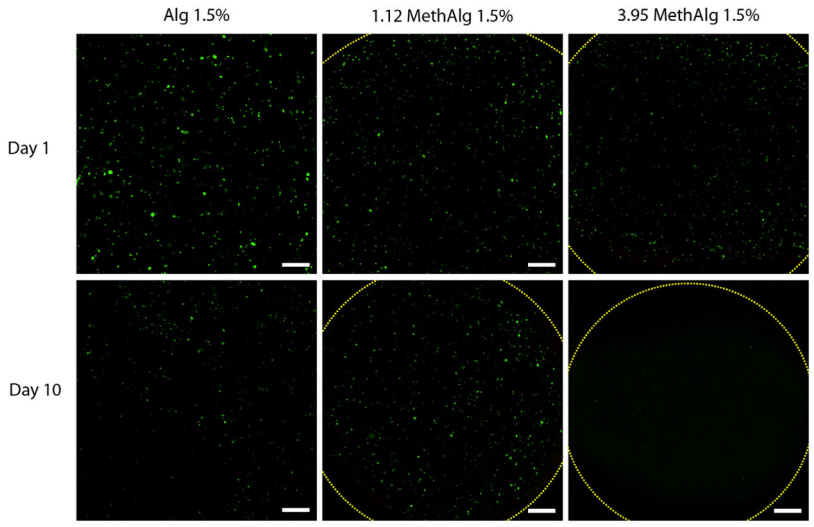

Fig. 8.

Live/Dead imaging of encapsulated MIN6 cells in dual crosslinked alginate hydrogels *in vitro*. Total number of cells appear to decrease from day 1 to day 10 for all groups tested. Dashed lines represents margins of the beads. Scale bar represents 200 μm.

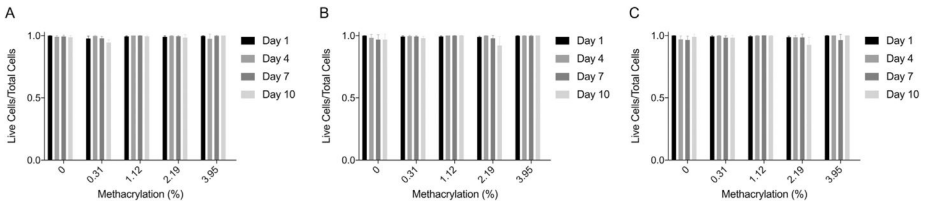

Fig. 9.

Quantitative live dead values for A) 1.5%, B) 1.8%, and C) 2.0% concentrations as a function of methacrylation efficiency for day 1, 4, 7, and 10. Cells within microbeads remained viable (>90%) up to 10 days for all formulations.

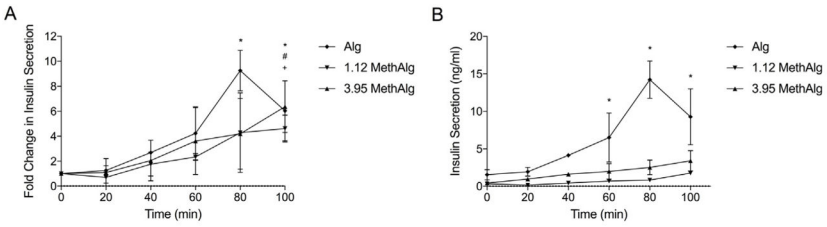

Fig. 10.

Insulin secretion of MIN6 cells encapsulated within ionically and covalently crosslinked alginate microbeads plotted both as A) fold change per time and B) concentration (ng/ml) per time. Insulin secretion increased with time for all formulations. *Denotes statistical difference ($p \leq .05$) for Alg when compared to time 0. #Denotes statistical difference ($p \leq .05$) for 1.12 MethAlg when compared to time 0. +Denotes statistical difference ($p \leq .05$) for 3.95 MethAlg when compared to time 0.

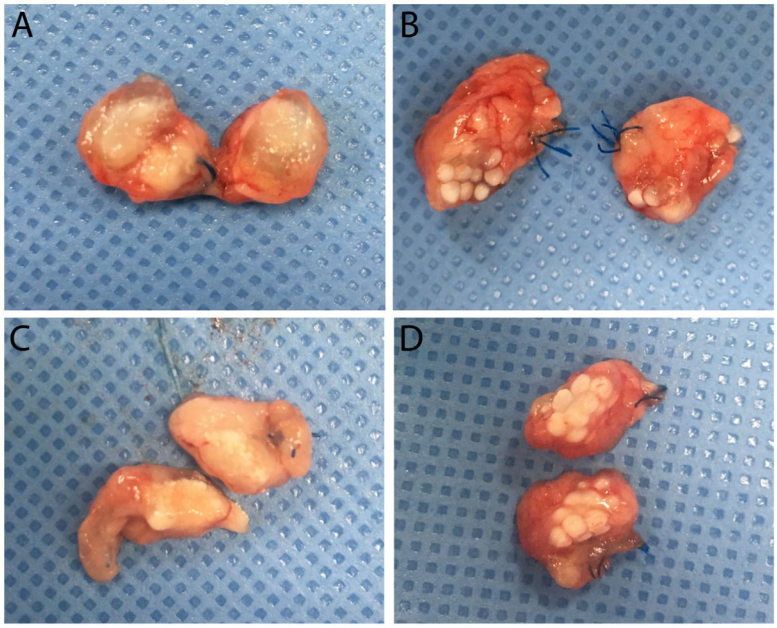

Fig. 11.

Representative images of bisected omentum harvested from animals receiving control (a, c) or methacrylated (1.12%; b, d) alginate microbeads. Pouches were harvested 1 week (a, b) or 3 weeks (c, d) after implantation.

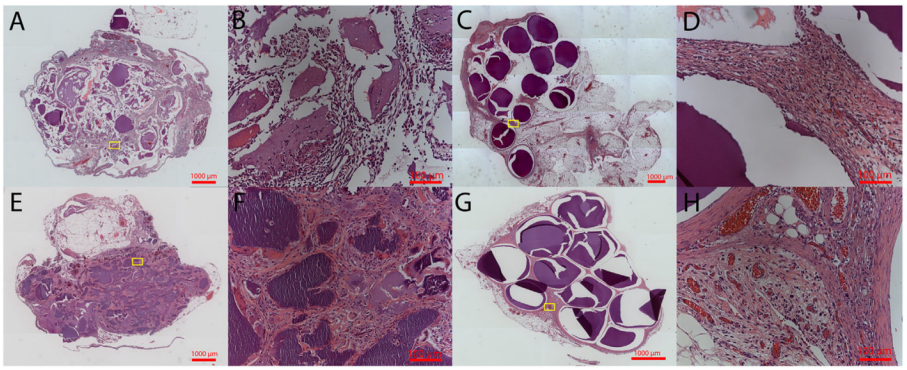

Fig. 12.

Hematoxylin and Eosin staining for control (A, B, E, F) and 1.12% ME (C, D, G, H) at 1 week (A, B, C, D) and 3 weeks (E, F, G, H). Low (5×) (A, C, E, G) and high (20×) (B, D, F, H) magnification are shown. Intact microbeads are observed in the dual crosslinked group at 1 and 3 weeks, whereas fragments of beads are seen in ionically crosslinked microbeads.

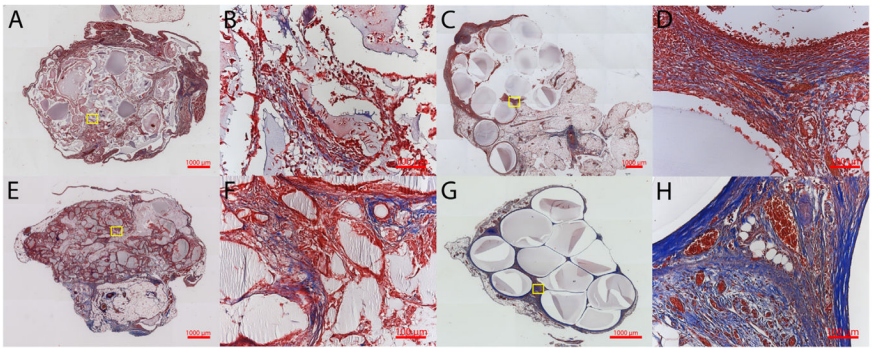

Fig. 13.

Masson's Trichrome staining for control (A, B, E, F) and 1.12% ME (C, D, G, H) at 1 week (A, B, C, D) and 3 weeks (E, F, G, H). Low (5×) (A, C, E, G) and high (20×) (B, D, F, H) magnification are shown. Inflammation surrounding the implants is observed for both ionically and dual crosslinked groups.

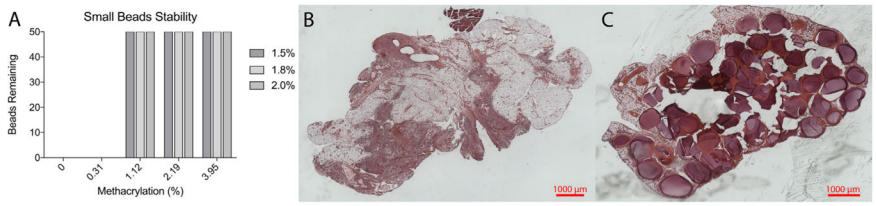

Fig. 14.

A) Number of microbeads remaining, out of 50, following exposure to mechanical forces for small beads (1344 μm). Hematoxylin and Eosin staining for B) control and C) 1.12 MethAlg at 1 week for small beads. Intact microbeads are observed in the dual crosslinked group at 1 week, whereas no beads are observed in the ionically crosslinked microbeads.